

Anomalous current fluctuations from Euler hydrodynamics

Takato Yoshimura^{1,2,*} and Žiga Krajnik^{3,†}

¹All Souls College, Oxford OX1 4AL, U.K.

²Rudolf Peierls Centre for Theoretical Physics, University of Oxford, 1 Keble Road, Oxford OX1 3NP, U.K.

³Department of Physics, New York University, 726 Broadway, New York, NY 10003, USA

We consider the hydrodynamic origin of anomalous current fluctuations in a family of stochastic charged cellular automata. Using ballistic macroscopic fluctuation theory, we study both typical and large fluctuations of the charge current and reproduce microscopic results which are available for the deterministic single-file limit of the models. Our results indicate that in general initial fluctuations propagated by Euler equations fully characterize anomalous fluctuations on both scales. In the stochastic case, we find an additional contribution to typical fluctuations and conjecture the functional form of the typical probability distribution, which we confirm by numerical simulations.

Introduction.—Statistical physics aims to describe universal behaviors emerging from interactions of a large number of microscopic degrees of freedom. While traditionally the main focus has been equilibrium physics, in recent years it has been appreciated that out-of-equilibrium properties of the system can also display rich universal behaviors. A prominent tool that describes such physics is macroscopic fluctuations theory (MFT) [1], which captures large fluctuations of driven diffusive systems. The validity of MFT has been verified for a variety of systems [2–5] and also on quantum simulators [6], but large fluctuations in these systems usually behave in a regular way with finite scaled cumulants of observables. This naturally raises the question of whether there exists systems that break such regularity and support new dynamical phenomena.

Recent numerical studies have found dynamical criticality and anomalous spin fluctuations in integrable spin chains [7, 8], which have also been probed experimentally using superconducting qubits [9]. While the mechanism responsible for anomalous spin fluctuations remains to be clarified, an exact calculation of fluctuations in a deterministic charged cellular automaton [10] provided a basic example of dynamical criticality in a deterministic many-body system. The procedure has been generalized to a wider class of single-file dynamics, which was explored in Refs. [11–16]. Furthermore, anomalous fluctuations have also been observed in the easy-axis regime of an integrable spin chain [8, 17] and other systems including Dirac fluids [18] and stochastic processes [19], hinting at a more general setting supporting anomalous fluctuations.

Motivated by these, in this Letter, we provide a full hydrodynamic framework to understand the emergence of anomalous charge fluctuations in a family of stochastic charged cellular automata (SCCA), which was first introduced in Ref. [20] and reduces to the model studied in Ref. [10] in the single-file (deterministic) limit. The main tool for the analysis is ballistic MFT (BMFT) [21, 22], which is a generalization of MFT for systems that support ballistic transport, and we employ it to characterize both typical and large fluctuations. The simple three-mode hydrodynamic structure allows for an exact solu-

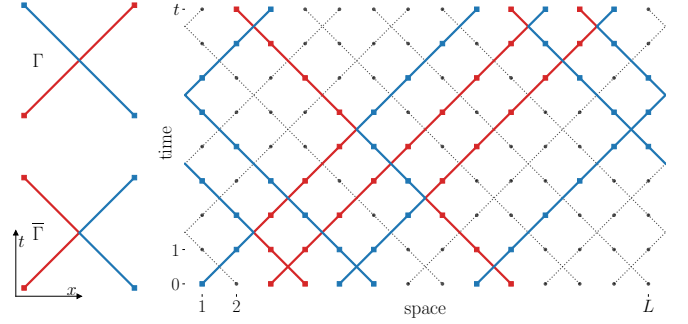


Figure 1. (left) Stochastic particle scattering in the two-particle sector of the local two-body map Φ . Particles with positive/negative charge (red/blue squares) either cross (top left) with probability Γ or are elastically reflected (bottom left) with probability $\bar{\Gamma}$. Particle worldlines (colored lines) shown for clarity. (right) Many-body dynamics of charged particles and vacancies (black circles) in discrete space-time. Particles move along diagonals except when they encounter another particle when they scatter stochastically.

tion of BMFT equations, showing that large charge fluctuations are identical in the whole family of SCCA. While BMFT is in principle applicable only to large fluctuations, we also demonstrate that an approach based on the same idea, which is that current fluctuations are solely determined by initial fluctuations transported by Euler hydrodynamics, accurately describes typical fluctuations in the single-file limit, recovering the microscopic result [10]. Interestingly, unlike large fluctuations, it turns out that typical fluctuations depend on the stochasticity of dynamics. Based on numerical simulations, we conjecture a form of the corresponding typical distribution at half-filling.

The model.—We consider a family of SCCA on a one-dimensional lattice of $L \in 2\mathbb{N}$ sites. The lattice configuration at fixed time $t \in \mathbb{Z}$ is given by strings $s^t \equiv s_L^t s_{L-1}^t \dots s_1^t$ of symbols $s_x^t \in \{\emptyset, -, +\}$, which correspond to vacancies and negatively or positively charged particles, respectively. Local symbol dynamics are given by a one-parameter stochastic two-body map $(s'_L, s'_R) = \Phi(s_L, s_R)$ which encodes the following dynamical rules

$(\emptyset, \emptyset) \rightarrow (\emptyset, \emptyset)$, $(\emptyset, c) \leftrightarrow (c, \emptyset)$ while $(c, c') \rightarrow (c', c)$ with probability $0 \leq \Gamma \leq 1$ and $(c, c') \rightarrow (c, c')$ with probability $\bar{\Gamma} \equiv 1 - \Gamma$ where $c, c' \in \{-, +\}$, see Figure 1. We note that the dynamics can be understood as a composition of a stochastic six-vertex model in the particle-particle sector with free dynamics in the remaining sectors, see the Supplemental Material (SM) [23] for details.

The many-body dynamics is realized as a ‘brickwork’ circuit obtained by imposing periodic boundary conditions, $s_x^t = s_{L+x}^t$, and coupling alternating sites as $\mathbf{s}^{2t+2} = \Phi^{\text{odd}}(\mathbf{s}^{2t+1})$ and $\mathbf{s}^{2t+1} = \Phi^{\text{even}}(\mathbf{s}^{2t})$, where

$$\Phi^{\text{odd}} = \prod_{x=1}^{L/2} \Phi_{2x-1, 2x}, \quad \Phi^{\text{even}} = \prod_{x=1}^{L/2} \Phi_{2x, 2x+1} \quad (1)$$

and $\Phi_{x, x+1}$ acts non-trivially only on sites x and $x+1$, see Figure 1 for a sample many-body trajectory. For $\Gamma = 0$ and $\Gamma = 1$ the dynamics is deterministic and corresponds to single-file [10, 11, 24, 25] and free dynamics respectively.

While the SCCA are super-integrable and support an exponential (in L) number of local conserved quantities [26], we presently restrict our study to a (closed) subset of conserved charges, comprising the number of right and left moving particles \hat{Q}_{\pm} and the total charge \hat{Q}_c , all of which are given as sums of local densities $\hat{Q}_i(\mathbf{s}) = \sum_{x=1}^L \hat{q}_{x,t}^i(\mathbf{s})$ where $i \in \mathcal{I} \equiv \{+, -, c\}$ and $\hat{\bullet}$ indicates a microscopic quantity, see SM [23] for details on charge densities and discrete space-time continuity relations.

We consider generalized Gibbs ensembles (GGEs) of the form $\mathbb{P}(\mathbf{s}) = \exp[\beta^i \hat{Q}_i(\mathbf{s})] / \sum_{\mathbf{s}'} \exp[\beta^i \hat{Q}_i(\mathbf{s}')]]$, where repeated upper and lower indices indicate summation. The average of an observable $o(\mathbf{s})$ is accordingly $\langle o \rangle = \sum_{\mathbf{s}} \mathbb{P}(\mathbf{s}) o(\mathbf{s})$. Identifying the ensemble parameters as $\rho_{\pm} = [1 + e^{-\beta_{\pm}} / (2 \cosh \beta_c)]^{-1}$, $b = \tanh \beta_c$, the ensemble factorizes $\mathbb{P}(\mathbf{s}) = \prod_{x=1}^{L/2} p_{-}(s_{2x+1}) p_{+}(s_{2x})$ in terms of normalized one-site measures $p_{-}(\pm) = \rho_{-} \frac{1 \pm b}{2}$, $p_{+}(\pm) = \rho_{+} \frac{1 \pm b}{2}$, $p_{\pm}(\emptyset) = \bar{p}_{\pm}$ with $0 \leq \rho_{\pm} \leq 1$ and $\bar{p}_{\pm} \equiv 1 - \rho_{\pm}$ the densities of right/left movers and vacancies on right/left running diagonals, respectively.

Hydrodynamics.—The hydrodynamics of the system turns out to have a simple structure with densities of left and right moving particles $\varrho_{\pm}/2$ and charge ϱ_c forming a *closed set of hydrodynamic equations*. To study charge transport (in the chosen GGE) it is then sufficient to consider the hydrodynamics of only these three charges unlike in a standard integrable systems where all charges must be included.

The three-mode hydrodynamic equations of the SCCA are obtained by evaluating the flux jacobian

$$[\mathbf{A}[\underline{\varrho}]]_i^j = \frac{\partial j_i[\underline{\varrho}]}{\partial \varrho_j} = \begin{pmatrix} 1 & 0 & 0 \\ 0 & -1 & 0 \\ b\rho_{-}/\rho & -b\rho_{+}/\rho & v \end{pmatrix} \quad (2)$$

where three modes are labeled by $\rho_1 = \rho_{+}/2$, $\rho_2 = \rho_{-}/2$,

$\rho_3 = \rho_c$ and the charge velocity v is given by $v = p/\rho$ with $\rho = \rho_1 + \rho_2$, $p = \rho_1 - \rho_2$ the particle density and momentum respectively (see SM [23] for the derivation) and $j_i[\underline{\varrho}]$ is the average current defined via the continuity equation $\partial_t \varrho_i + \partial_x j_i[\underline{\varrho}] = 0$. Here, ϱ_i is a space-time dependent density and the underline implies that the quantity is multicomponent. Charge inertness and chiral factorization of the dynamics amount to free ballistic propagation of the left and right movers $\partial_t(\varrho_{\pm}/2) \pm \partial_x(\varrho_{\pm}/2) = 0$. On the other hand, charge transport is affected by particle dynamics and the Euler equation is of the form

$$\partial_t \varrho_c + \partial_x(v \varrho_c) = 0. \quad (3)$$

A system of three-mode hydrodynamic equations similar to Eq. (3) along with the free chiral equations for ϱ_{\pm} was also recently derived for Dirac fluids by keeping only the most relevant terms based on symmetry considerations in Ref. [18]. In the present case, the hydrodynamic equations are obtained using the exact flux jacobian Eq. (2), and interestingly, are completely insensitive to the crossing probability Γ . That said, as we will see later, typical fluctuations do turn out to depend nontrivially on Γ . Before discussing this dependence, we first study large fluctuations of the SCCA, which can be fully characterized using only Euler hydrodynamic data.

Anomalous charge FCS from BMFT.—The central object in the study of fluctuations is the generating function $\langle e^{i\lambda \hat{J}(t)} \rangle = \int d\lambda e^{i\lambda J} \mathcal{P}(J|t)$ given by the probability distribution $\mathcal{P}(J|t)$ of time-integrated charge current $\hat{J}(t) = \int_0^t dt' \hat{j}_c(0, t')$. While the scale on which *typical fluctuations* take place $\hat{J}(t) \sim t^{1/2z}$ is set by the variance $\langle [\hat{J}(t)]^2 \rangle^c \sim t^{1/z}$, large (atypical) fluctuations occur on the scale $\hat{J}(t) \sim t$ with a probability distribution governed by a large deviation principle $\mathcal{P}(J = jt|t) \asymp e^{-tI(j)}$ where $I(j)$ is the large deviation rate function. The rate function is related to the *scaled cumulant generating function* (SCGF)

$$F(\lambda) = \lim_{t \rightarrow \infty} t^{-1} \log \langle e^{\lambda \hat{J}(t)} \rangle \quad (4)$$

via the Legendre transform $I(j) = \max_{\lambda \in \mathbb{R}} [\lambda j - F(\lambda)]$. We now compute the charge SCGF in the SCCA explicitly using BMFT.

The fundamental postulate of BMFT is that large fluctuations of the initial state are propagated according to Euler equations in space-time, thereby governing the large-scale dynamics at later times. The idea is implemented by writing the generating function as

$$\langle e^{\lambda \hat{J}(\tau)} \rangle = \int_{(\mathbb{S})} \mathcal{D}\underline{\varrho}(\cdot, \cdot) \mathcal{D}\underline{H}(\cdot, \cdot) e^{-\tau S[\underline{\varrho}, \underline{H}]}, \quad (5)$$

where the functional integral is performed over the space of functions supported on the space-time region $\mathbb{S} = \mathbb{R} \times [0, 1]$, and the densities $\varrho_i(x, t)$ are the *fluctuating*

mesoscopic densities evaluated at the Euler-scale coordinates $(\tau x, \tau t)$, i.e. $\varrho_i(x, t) = \hat{\varrho}_i(\tau x, \tau t)$. The auxiliary field \underline{H} in Eq. (6) ensures that the fluctuating fields always satisfy the hydrodynamic equations, which in turn gives the BMFT action $S[\underline{\varrho}, \underline{H}]$

$$S[\underline{\varrho}, \underline{H}] = -J(1) + \mathcal{F}[\underline{\varrho}(\cdot, 0)] + \int_{\mathbb{S}} dx dt H^i (\partial_t \varrho_i + \partial_x j_i), \quad (6)$$

where $J(1) = \int_0^1 dt j_c(0, t)$ is the time-integrated current and $\mathcal{F}[\underline{\varrho}(\cdot, 0)]$ is the rate function of initial fluctuating densities

$$\mathcal{F}[\underline{\varrho}(\cdot, 0)] = \int_{\mathbb{R}} dx ((\beta^i(x, 0) - \beta^i) \varrho_i(x, 0) - f + f(x, 0)), \quad (7)$$

with Lagrange multipliers $\beta^i(x, 0)$, the free energy density $f(x, 0)$ associated with the initial fluctuating density profile $\underline{\varrho}(\cdot, 0)$, and the background free energy f . The saddle point of Eq. (5) now gives the BMFT equations

$$\lambda \delta_c^i \Theta(x) - \beta^i + \beta^i(x, 0) - H^i(x, 0) = 0, \quad (8)$$

$$\lambda \delta_c^i \Theta(x) - H^i(x, 1) = 0, \quad (9)$$

$$\partial_t \beta^i(x, t) + [A^T]^i_j(x, t) \partial_x \beta^j(x, t) = 0, \quad (10)$$

$$\partial_t H^i(x, t) + [A^T]^i_j(x, t) \partial_x H^j(x, t) = 0, \quad (11)$$

where $\Theta(x)$ is the Heaviside step function. In terms of the solution $\underline{\beta}^{(\lambda)}(x, t)$ of the BMFT equations, the SCGF is computed as [21]

$$F(\lambda) = \int_0^\lambda d\lambda' \int_0^1 dt j_c[\underline{\varrho}^{(\lambda')}(0, t)] \quad (12)$$

where $\underline{\varrho}^{(\lambda)}(x, t) = \underline{\varrho}[\underline{\beta}^{(\lambda)}(x, t)]$. Although solving BMFT equations is in general a formidable task even for (interacting) integrable systems, the simple hydrodynamic structure of the SCCA allows us to find their exact solution; see SM [23] for details. For $\beta^\pm = \beta$ and $t \in (0, 1)$ the solution along the ray $x = 0$ reads

$$\beta^{(\lambda), c}(0, t) = \beta^c(\lambda) = \beta^c + |\lambda| \operatorname{sgn} b, \quad (13)$$

$$\beta^{(\lambda), \pm}(0, t) = \beta - 2\Theta(\mp \lambda b) \log \left[\frac{\cosh \beta^c(\lambda)}{\cosh \beta^c} \right], \quad (14)$$

which, using Eq. (12), also gives the SCGF

$$F(\lambda) = \frac{1}{2} \log [1 + \Delta^2 (\mu_b + \mu_b^{-1} - 2)] \quad (15)$$

where $\Delta^2 = \rho(1 - \rho)$ and $\mu_b = \cosh \lambda + |b| \sinh |\lambda|$. This coincides precisely with the microscopic result obtained in [10] up to prefactor 1/2 due to a different convention for the unit of time.

As was also observed in Ref. [10], the SCGF Eq. (15) is anomalous in that the scaled higher cumulants $c_{2n>4} = \lim_{t \rightarrow \infty} t^{-1} \langle [\hat{J}(t)]^{2n} \rangle^c$ are singular. BMFT clarifies the physical origin of this anomalous behavior: since the

normal mode $b(x, t)$ of the charge $\varrho_c(x, t)$ travels along the ray $x = 0$, fluctuations along $x = 0$ proliferate and thereby render clustering of connected charge current correlations algebraic in time [27]. While such a scenario generally results in superdiffusion [28], it is avoided here due to the charge conjugation symmetry of the system [11]. In general, we expect that, for a charge in the system to show anomalous fluctuations, it has to have a vanishing velocity in equilibrium (usually afforded by a \mathbb{Z}_2 symmetry of the charge) and other modes should be independent of their own velocities (i.e. no self-coupling), which would otherwise induce superdiffusion of the charge as in the heat mode with the 5/3-Levy exponent in anharmonic chains [28]. It is also reasonable to assume that anomalous fluctuations are robust away from charge inertness, but a more precise analysis of such a situation is beyond the scope of the present Letter.

To our knowledge, the above solution is the first exact solution of full BMFT equations in an interacting model and therefore serves as an independent check of their validity. Furthermore, Eqs. (13) and (14) match the solution of the flow equation in ballistic fluctuation theory (see SM) [27, 29], corroborating the identification advocated in Ref. [21].

Note that Eq. (15) is valid for any value of $b \in (-1, 1)$, including $b = 0$, where the dynamical exponent becomes $z = 2$. On the other hand, for typical fluctuations the two cases $b \neq 0$ and $b = 0$ have to be treated separately since the dynamical exponents in the two cases differ. However, it turns out that, in the single-file (i.e., deterministic) limit $\Gamma = 0$, the underlying mechanism, namely that initial fluctuations evolving according to the Euler equations fully determine charge current fluctuations, remains true even for typical fluctuations.

Typical fluctuations of deterministic dynamics from Euler hydrodynamics.—The probability distribution of typical charge fluctuations $\hat{J}(t) \sim t^{1/2z}$ is given by

$$\mathcal{P}(J t^{-1/2z} | t) = \int_{\mathbb{R}} \frac{d\lambda}{2\pi} e^{-i\lambda J t^{-1/2z}} \langle e^{i\lambda \hat{J}(t)} \rangle, \quad (16)$$

which converges to $\mathcal{P}_{\text{typ}}(j) = \lim_{t \rightarrow \infty} t^{1/2z} \mathcal{P}(J = j t^{1/2z} | t)$. We now evaluate Eq. (16) using only Euler hydrodynamic data, focusing on the single-file limit $\Gamma = 0$, which has been discussed extensively in Refs. [10–12].

Recall that, the main ideas of both MFT and BMFT, which describe large fluctuations, hinge on the postulate that the generating function $\langle e^{i\lambda \hat{J}(t)} \rangle$ can be expressed solely in terms of diffusive- or Euler-scale variables $\varrho_i(x, t)$, respectively, whose fluctuations are of order $O(1)$. Importantly, these fluctuating variables originate from atypical initial fluctuations described by Eq. (7), which evolve in time according to their respective hydrodynamic equations.

Motivated by this, we argue that, for large times, *all contributions of the generating function to the integral in*

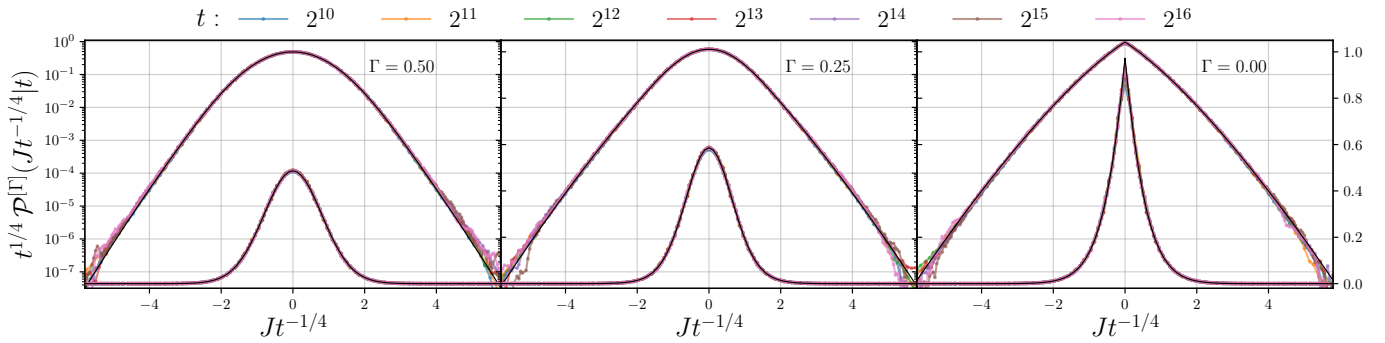


Figure 2. Finite-time typical distributions of the integrated charge current $t^{1/4}\mathcal{P}^{[\Gamma]}(Jt^{-1/4}|t)$ (colored lines) in linear and logarithmic scales at different Γ compared against distributions $\mathcal{P}_{\text{typ}}^{[\Gamma]}$ (20) (black lines) with ω and σ as fitting parameters, best-fit values reported in the SM [23]. Simulation parameters: $\rho = 1/2$, $b = 0$, $L = 2^{20}$, $t_{\text{max}} = 2^{16}$, 5×10^3 samples.

Eq. (16) for $\Gamma = 0$ are captured by fluctuating variables $\varrho_i(x, t) = \hat{\varrho}_i(\tau^{1/z}x, \tau t)$, $\tau \gg 1$, that can be obtained by propagating initial typical fluctuations:

$$\varrho_i(x, 0) \simeq \rho_i + \tau^{-1/2z} \delta\varrho_i(x, 0), \quad (17)$$

where ρ_i is the initial average density and $\delta\varrho_i(x, 0)$ is a field with $O(1)$ fluctuations.

The assertion that such fluctuations are always transported by the Euler equations regardless of the dynamical exponent stems from the observation that the only source of typical current fluctuations in the SCCA are the interactions of ballistically-propagating initial typical fluctuations. A similar observation was recently also made for Dirac fluids in Ref. [18]. This is in fact in the same spirit as *diffusion from convection*, which is known to be the only contribution to the diffusion constants in integrable systems [30–32] (we show that this is also the case in the SCCA in SM) and is generically also present even in non-integrable systems, provided that the eigenvalues of the flux jacobian \mathbf{A} are non-degenerate [33].

To illustrate the idea, we focus on the case of half-filling $b = 0$ and leave the details and $b \neq 0$ for the SM. Since in this case the dynamical exponent of charge transport is $z = 2$, the fluctuating fields $\varrho_i(x, t)$ need to be rescaled to the diffusive coordinates $\varrho_i(x, t) = \hat{\varrho}_i(\sqrt{\tau}x, \tau t)$ with the associated currents $j_i(x, t) = \sqrt{\tau}\hat{j}_i(\sqrt{\tau}x, \tau t)$. The fields $\varrho_i(x, t)$ then fluctuate initially as $\varrho_i(x, 0) \simeq \rho_i + \tau^{-1/4}\delta\varrho_i(x, 0)$, where $\delta\varrho_i(x, 0)$ is Gaussian distributed as $\langle \delta\varrho_i(x, 0)\delta\varrho_j(y, 0) \rangle = \mathbf{C}_{ij}\delta(x - y)$ with the susceptibility matrix $\mathbf{C}_{ij} = \partial\rho_i/\partial\beta^j$ (see SM for the explicit expression). The fluctuating particle fields $\delta\varrho_{\pm}(x, 0)$ are then transported by the Euler equation $\partial_t\delta\varrho_{\pm}(x, t) \pm \sqrt{\tau}\partial_x\delta\varrho_{\pm}(x, t) = 0$, which can be solved as $\delta\varrho_{\pm}(x, t) \simeq \rho_{\pm} + \tau^{-1/4}\delta\varrho_{\pm}(x \mp \sqrt{\tau}t, 0)$. Likewise the charge field $\delta\varrho_c(x, t)$ also fluctuates as $\delta\varrho_c(x, t) \simeq \tau^{-1/4}\delta\varrho_c(x - X_d(t), 0)$ where $X_d(t)$ is the characteristics that satisfies $dX_d(t)/dt = \sqrt{\tau}v(X_d(t), t)$. With these we obtain the leading behavior of the fluctuating charge current at the origin $j_c(0, t) \simeq \tau^{-1/4}\partial_t \int_0^{X_d(t)} dx \delta\varrho_c(-x, 0)$, which in

turn allows us to write down the functional integral that describes the contribution to the typical fluctuations by these fields

$$\langle e^{\lambda J_c(\tau)} \rangle \simeq \frac{1}{Z} \int_{(\mathbb{R})} \mathcal{D}\underline{\delta\varrho}(\cdot, 0) e^{-\frac{C^{ij}}{2} \int_{\mathbb{R}} dx \delta\varrho_i(x, 0)\delta\varrho_j(x, 0)} \times e^{\lambda\tau^{1/4} \int_0^{X_d(1)} dx \delta\varrho_c(-x, 0)}, \quad (18)$$

where $C^{ij} = [C^{-1}]_{ij}$ and Z is the normalization factor of the initial probability distribution. This integral can be performed exactly (see SM), yielding the non-Gaussian distribution

$$\mathcal{P}_{\text{typ}}(j) = \frac{1}{2\pi\Delta} \int_{\mathbb{R}} \frac{du}{\sqrt{|u|}} e^{-\frac{u^2}{2\Delta^2} - \frac{j^2}{2|u|}}, \quad (19)$$

which matches the result reported in Ref. [10]. The breakdown of Gaussianity in Eq. (19) can be understood by noting which fluctuating fields are responsible for charge current fluctuations. At half-filling, it follows from Eq. (18) that charge fluctuations $\delta\varrho_c(x, t)$ that travel along the characteristics $X_d(t)$ and cross $x = 0$ between $t = 0$ and $t = \tau$ contribute to current fluctuations. Since charge fluctuations are transported non-linearly, Gaussianity of initial fluctuations is no longer preserved and typical fluctuation become non-Gaussian. The situation changes dramatically away from half-filling, i.e. for $b \neq 0$ where only particle fluctuations $\delta\varrho_{\pm}(x, t)$ emanating along light cones contribute to charge current fluctuations. Since particle fluctuations are transported linearly, Gaussianity of initial fluctuations is preserved during the dynamics, giving rise to Gaussian typical fluctuations (see SM for details).

Typical fluctuations of stochastic dynamics.—The distribution (19) features a cusp at the origin. Numerical simulations for $\Gamma > 0$ at half-filling indicate that the cusp is rounded off with stochastic crossings while the distribution remains non-Gaussian. This motivates a generalization of the single-file distribution (19) of the form

$$\mathcal{P}_{\text{typ}}^{[\Gamma]}(j) = \frac{1}{2\pi\sigma} \int_{\mathbb{R}} \frac{du}{\sqrt{u^2 + \omega^2}} e^{-\frac{u^2}{2\sigma^2} - \frac{j^2}{2\sqrt{u^2 + \omega^2}}}, \quad (20)$$

which reduces to the single-file distribution (19) as $\omega \rightarrow 0$ and to a Gaussian distribution (with variance ω) as $\omega \rightarrow \infty$. Treating ω and σ as Γ -dependent fitting parameters, the distribution (20) accurately captures the asymptotic typical distribution for $\Gamma \geq 0$ across 5 order of magnitude as shown in Fig. 2.

Conclusions.—We have studied anomalous charge current fluctuations in a family of stochastic cellular automata and characterized both large and typical fluctuations based only on Euler hydrodynamics, reproducing the microscopic results obtained in Ref. [10] when specializing to the single-file (i.e. deterministic) limit $\Gamma = 0$. The key insight is that initial fluctuations, carried by Euler hydrodynamics, fully control fluctuations both on the typical and large scales in the single-file case. To implement the idea, we employed BMFT to compute the SCGF and proposed a BMFT-based approach to describe typical fluctuations induced by initial Gaussian fluctuations (in a forthcoming work Ref. [34], it is also shown how BMFT provides the full diffusive-order hydrodynamic equation, where the long-range correlations predicted by BMFT are the source of diffusive-order terms). Following Ref. [18], our work further clarifies the hydrodynamic origin of anomalous fluctuations, which we believe is generic among systems that exhibit anomalous fluctuations.

While initial fluctuations remain the only source of large fluctuations even in the stochastic case $\Gamma \neq 0$, it turns out that typical fluctuations are nontrivially influenced by the presence of stochasticity, which is not prescribed by initial fluctuations. We expect that stochasticity induces normal diffusion, and it would be very interesting to reproduce Eq. (20) by extending the formalism we introduced to incorporate normal diffusion. The observation of the distribution (19) in a classical spin chain [8] therefore supports the absence of normal diffusion in the easy-axis regime [35, 36]. Other important directions would be to obtain the exact FCS of the SCCA via microscopic computations and to establish a scattering description of thermodynamics, as recently obtained for classical integrable spin chains [37].

Acknowledgements.—We thank Bruno Bertini, Benjamin Doyon, Sarang Gopalakrishnan, Enej Ilievski, Katja Klobas, Marcin Mierzejewski, Peter Prelovšek, Tomaž Prosen, and Herbert Spohn for useful discussions. We are also grateful to Alvis Bastianello for his comments on the manuscript. ŽK is supported by the Simons Foundation as a Junior Fellow of the Simons Society of Fellows (1141511). This paper is dedicated to the memory of Marko Medenjak (1990-2022).

* takato.yoshimura@physics.ox.ac.uk

† ziga.krajnik@nyu.edu

[1] L. Bertini, A. De Sole, D. Gabrielli, G. Jona-Lasinio, and

- C. Landim, Macroscopic fluctuation theory, *Rev. Mod. Phys.* **87**, 593 (2015).
- [2] T. Bodineau and B. Derrida, Distribution of current in nonequilibrium diffusive systems and phase transitions, *Phys. Rev. E* **72**, 066110 (2005).
- [3] B. Derrida and A. Gerschenfeld, Current Fluctuations in One Dimensional Diffusive Systems with a Step Initial Density Profile, *Journal of Statistical Physics* **137**, 978–1000 (2009).
- [4] P. L. Krapivsky, K. Mallick, and T. Sadhu, Tagged Particle in Single-File Diffusion, *Journal of Statistical Physics* **160**, 885–925 (2015).
- [5] K. Mallick, H. Moriya, and T. Sasamoto, Exact Solution of the Macroscopic Fluctuation Theory for the Symmetric Exclusion Process, *Phys. Rev. Lett.* **129**, 040601 (2022).
- [6] J. F. Wienand, S. Karch, A. Impertro, C. Schweizer, E. McCulloch, R. Vasseur, S. Gopalakrishnan, M. Aidelsburger, and I. Bloch, Emergence of fluctuating hydrodynamics in chaotic quantum systems (2023), [arXiv:2306.11457 \[cond-mat.quant-gas\]](https://arxiv.org/abs/2306.11457).
- [7] Ž. Krajnik, E. Ilievski, and T. Prosen, Absence of Normal Fluctuations in an Integrable Magnet, *Phys. Rev. Lett.* **128**, 090604 (2022).
- [8] Ž. Krajnik, J. Schmidt, E. Ilievski, and T. Prosen, Dynamical Criticality of Magnetization Transfer in Integrable Spin Chains, *Phys. Rev. Lett.* **132**, 017101 (2024).
- [9] E. Rosenberg *et al.*, Dynamics of magnetization at infinite temperature in a Heisenberg spin chain, *Science* **384**, 48–53 (2024).
- [10] Ž. Krajnik, J. Schmidt, V. Pasquier, E. Ilievski, and T. Prosen, Exact Anomalous Current Fluctuations in a Deterministic Interacting Model, *Phys. Rev. Lett.* **128**, 160601 (2022).
- [11] Ž. Krajnik, J. Schmidt, V. Pasquier, T. Prosen, and E. Ilievski, Universal anomalous fluctuations in charged single-file systems, *Physical Review Research* **6**, 10.1103/physrevresearch.6.013260 (2024).
- [12] Ž. Krajnik, Single-file dynamics with general charge measures, [arXiv:2401.14378](https://arxiv.org/abs/2401.14378) (2024).
- [13] B. Altshuler, R. Konik, and A. Tsvetlik, Low temperature correlation functions in integrable models: Derivation of the large distance and time asymptotics from the form factor expansion, *Nuclear Physics B* **739**, 311–327 (2006).
- [14] J. Feldmeier, W. Witczak-Krempa, and M. Knap, Emergent tracer dynamics in constrained quantum systems, *Phys. Rev. B* **106**, 094303 (2022).
- [15] M. Kormos, D. Vörös, and G. Zaránd, Finite-temperature dynamics in gapped one-dimensional models in the sine-Gordon family, *Phys. Rev. B* **106**, 205151 (2022).
- [16] K. Bidzhiev, M. Fagotti, and L. Zadnik, Macroscopic Effects of Localized Measurements in Jammed States of Quantum Spin Chains, *Phys. Rev. Lett.* **128**, 130603 (2022).
- [17] S. Gopalakrishnan, A. Morningstar, R. Vasseur, and V. Khemani, Distinct universality classes of diffusive transport from full counting statistics, *Phys. Rev. B* **109**, 024417 (2024).
- [18] S. Gopalakrishnan, E. McCulloch, and R. Vasseur, Non-Gaussian diffusive fluctuations in Dirac fluids (2024), [arXiv:2401.05494](https://arxiv.org/abs/2401.05494).
- [19] E. McCulloch, R. Vasseur, and S. Gopalakrishnan, Ballistic modes as a source of anomalous charge noise (2024),

- arXiv:2407.03412 [cond-mat.stat-mech].
- [20] K. Klobas, M. Medenjak, and T. Prosen, Exactly solvable deterministic lattice model of crossover between ballistic and diffusive transport, *Journal of Statistical Mechanics: Theory and Experiment* **2018**, 123202 (2018).
- [21] B. Doyon, G. Perfetto, T. Sasamoto, and T. Yoshimura, Ballistic macroscopic fluctuation theory, *SciPost Phys.* **15**, 136 (2023).
- [22] B. Doyon, G. Perfetto, T. Sasamoto, and T. Yoshimura, Emergence of Hydrodynamic Spatial Long-Range Correlations in Nonequilibrium Many-Body Systems, *Phys. Rev. Lett.* **131**, 027101 (2023).
- [23] Supplemental Material.
- [24] M. Medenjak, K. Klobas, and T. Prosen, Diffusion in Deterministic Interacting Lattice Systems, *Physical Review Letters* **119**, 10.1103/physrevlett.119.110603 (2017).
- [25] M. Medenjak, V. Popkov, T. Prosen, E. Ragoucy, and M. Vanicat, Two-species hardcore reversible cellular automaton: matrix ansatz for dynamics and nonequilibrium stationary state, *SciPost Phys.* **6**, 074 (2019).
- [26] T. Gombor and B. Pozsgay, Superintegrable cellular automata and dual unitary gates from Yang-Baxter maps, *SciPost Phys.* **12**, 102 (2022).
- [27] B. Doyon and J. Myers, Fluctuations in Ballistic Transport from Euler Hydrodynamics, *Annales Henri Poincaré* **21**, 255–302 (2019).
- [28] H. Spohn, Nonlinear Fluctuating Hydrodynamics for Anharmonic Chains, *Journal of Statistical Physics* **154**, 1191–1227 (2014).
- [29] J. Myers, M. J. Bhaseen, R. J. Harris, and B. Doyon, Transport fluctuations in integrable models out of equilibrium, *SciPost Phys.* **8**, 007 (2020).
- [30] J. De Nardis, D. Bernard, and B. Doyon, Hydrodynamic Diffusion in Integrable Systems, *Phys. Rev. Lett.* **121**, 160603 (2018).
- [31] J. D. Nardis, D. Bernard, and B. Doyon, Diffusion in generalized hydrodynamics and quasiparticle scattering, *SciPost Phys.* **6**, 49 (2019).
- [32] S. Gopalakrishnan, D. A. Huse, V. Khemani, and R. Vasseur, Hydrodynamics of operator spreading and quasiparticle diffusion in interacting integrable systems, *Phys. Rev. B* **98**, 220303(R) (2018).
- [33] M. Medenjak, J. D. Nardis, and T. Yoshimura, Diffusion from convection, *SciPost Phys.* **9**, 075 (2020).
- [34] L. Biagetti, J. De Nardis, B. Doyon, and F. Hübner, (2024), in preparation.
- [35] P. Prelovšek, S. El Shawish, X. Zotos, and M. Long, Anomalous scaling of conductivity in integrable fermion systems, *Phys. Rev. B* **70**, 205129 (2004).
- [36] P. Prelovšek, S. Nandy, Z. Lenarčič, M. Mierzejewski, and J. Herbrych, From dissipationless to normal diffusion in the easy-axis Heisenberg spin chain, *Phys. Rev. B* **106**, 245104 (2022).
- [37] A. Bastianello, Ž. Krajnik, and E. Ilievski, Landau-Lifschitz magnets: exact thermodynamics and transport, arXiv:2404.12106 (2024).

SUPPLEMENTARY MATERIAL FOR
 “ANOMALOUS CURRENT FLUCTUATIONS FROM EULER HYDRODYNAMICS”

Takato Yoshimura^{1,2}

¹All Souls College, Oxford OX1 4AL, U.K.

²Rudolf Peierls Centre for Theoretical Physics, University of Oxford, 1 Keble Road, Oxford OX1
3NP, U.K.

Žiga Krajnik³

³Department of Physics, New York University, 726 Broadway, New York, NY 10003, USA

I. STOCHASTIC CHARGED CELLULAR AUTOMATA

The configuration space of a a systems of $L \in \mathbb{N}$ sites C_L is spanned by strings

$$\mathbf{s} = s_L s_{L-1} \dots s_1 \tag{S1}$$

of symbols $s_x \in \{\emptyset, -, +\}$, which correspond to empty sites (vacancies) and negative/positive particles respectively. Local dynamics of the symbols are given by a one-parameter stochastic two-body map $(s'_L, s'_R) = \Phi(s_L, s_R)$ which encodes the following dynamical rules

$$(\emptyset, \emptyset) \rightarrow (\emptyset, \emptyset), \quad (\emptyset, c) \leftrightarrow (c, \emptyset), \quad (c, c') \rightarrow \begin{cases} (c', c), & \text{with probability } \Gamma, \\ (c, c'), & \text{with probability } \bar{\Gamma}, \end{cases} \quad c, c' \in \{-, +\}. \tag{S2}$$

where $0 \leq \Gamma \leq 1$ and $\bar{\Gamma} \equiv 1 - \Gamma$ are crossing and reflection probabilities respectively. Ordering the local basis $|s_L s_R\rangle$ as $(\emptyset\emptyset, \emptyset-, \emptyset+, -\emptyset, +\emptyset, --, -+, +- , ++)$, the local two-body map is given by a $3^2 \times 3^2$ bistochastic matrix

$$\langle s'_L s'_R | \Phi | s_L s_R \rangle = \left[\begin{array}{cc|cc} 1 & & & \\ & 1 & & \\ & & 1 & \\ \hline & 1 & & \\ & & 1 & \\ & & & \bar{\Gamma} & \Gamma \\ & & & \Gamma & \bar{\Gamma} \\ & & & & 1 \end{array} \right]. \tag{S3}$$

Note that the matrix (S3) is a (symmetric) stochastic six-vertex model in the particle-particle subspace and a swap in the vacancy-vacany and vacany-particles subspaces, corresponding to the

composition of a discrete-time symmetric simple exclusion process with otherwise freely propagating particles. The local dynamics is embedded into the many-body configuration space as

$$\Phi_{x,x+1} = \text{Id}^{\otimes(x-1)} \otimes \Phi \otimes \text{Id}^{\otimes(L-x-1)}, \quad (\text{S4})$$

where $\text{Id}(s) = s$ is a local unit map and we impose periodic boundary conditions, $x = x + L$. The full one propagator of many-body dynamics, $\mathbf{s}^{t+2} = \Phi^{\text{full}}(\mathbf{s}^t)$, of a system of even length $L \in 2\mathbb{N}$ consists of alternating even/odd steps

$$\Phi^{\text{full}} = \Phi^{\text{odd}}\Phi^{\text{even}}, \quad (\text{S5})$$

which further decompose as

$$\Phi^{\text{odd}} = \prod_{x=1}^{L/2} \Phi_{2x-1,2x}, \quad \Phi^{\text{even}} = \prod_{x=1}^{L/2} \Phi_{2x,2x+1}. \quad (\text{S6})$$

The dynamics (S5) for $\Gamma = 0$ and $\Gamma = 1$ are deterministic and correspond to single-file and free dynamics respectively. We exclude the free dynamics at $\Gamma = 1$ from the following analysis.

II. MAXIMUM ENTROPY ENSEMBLES AND THERMODYNAMICS

We consider maximum entropy measures with specified averages of left/right movers and charges which factorizes

$$\mathbb{P}(\mathbf{s}) = \prod_{x=1}^{L/2} p_{-}(s_{2x+1})p_{+}(s_{2x}), \quad (\text{S7})$$

in terms of normalized one-site measures

$$p_{-}(\pm) = \rho_{-} \frac{1 \pm b}{2}, \quad p_{+}(\pm) = \rho_{+} \frac{1 \pm b}{2}, \quad p_{\pm}(\emptyset) = \bar{\rho}_{\pm}, \quad (\text{S8})$$

with $0 \leq \rho_{\pm} \leq 1$ and $\bar{\rho}_{\pm} \equiv 1 - \rho_{\pm}$ the densities of right/left movers and vacancies respectively. The measure (S7) is an invariant measure for the many-body dynamics (S5), $\mathbb{P}(\mathbf{s}) = \mathbb{P}(\Phi^{\text{full}}(\mathbf{s}))$. It can be alternatively parametrized as a grand-canonical Gibbs ensemble

$$\mathbb{P}(\mathbf{s}) = \mathcal{Z}^{-1} \exp \left[\beta^i \hat{Q}_i(\mathbf{s}) \right], \quad (\text{S9})$$

with the index set $\mathcal{I} = \{-, +, c\}$. The conserved charges $\hat{Q}_i(\mathbf{s}) = \hat{Q}_i(\Phi^{\text{full}}(\mathbf{s}))$ are given as sums of local densities $\hat{q}_{x,t}^i$

$$\hat{Q}^i(\mathbf{s}) = \sum_{x=1}^L \hat{q}_{x,t}^i(\mathbf{s}), \quad (\text{S10})$$

with $\hat{q}_{x,t}^i(\mathbf{s}) = \hat{q}_{x,t}^i(s_x^t)$ and

$$\hat{q}_{x,t}^i(\emptyset) = 0, \quad \hat{q}_{x,t}^-(\pm) = \begin{cases} 0, & x+t \in 2\mathbb{Z}, \\ 1, & x+t \in 2\mathbb{Z}+1, \end{cases}, \quad (\text{S11})$$

$$\hat{q}_{x,t}^c(\pm) = \pm 1, \quad \hat{q}_{x,t}^+(\pm) = \begin{cases} 1, & x+t \in 2\mathbb{Z}, \\ 0, & x+t \in 2\mathbb{Z}+1, \end{cases}. \quad (\text{S12})$$

Local densities of conserved quantities satisfy a discrete continuity equation of the form

$$\frac{1}{2} (\hat{q}_{x,t+2}^i - \hat{q}_{x,t}^i) + \hat{j}_{x+1,t+1}^i - \hat{j}_{x,t+1}^i = 0, \quad (\text{S13})$$

with local current densities

$$\hat{j}_{x,t+1}^i = \frac{(-1)^x}{2} (\hat{q}_{x,t+1+(-1)^x}^i - \hat{q}_{x,t+1}^i). \quad (\text{S14})$$

The partition function $\mathcal{Z} = \sum_{\mathbf{s}} \exp[\beta^i \hat{Q}_i(\mathbf{s})]$ in Eq. (S9) evaluates to

$$\mathcal{Z} = \mathcal{Z}_-^{L/2} \mathcal{Z}_+^{L/2}, \quad (\text{S15})$$

where $\mathcal{Z}_{\pm} = 1 + 2e^{-\beta_{\pm}} \cosh \beta_c$. The corresponding equilibrium free energy per lattice site $f_{\text{eq}} = L^{-1} \log \mathcal{Z}$ reads

$$f_{\text{eq}}(\beta_-, \beta_+, \beta_c) = \frac{f_- + f_+}{2}, \quad (\text{S16})$$

with $f_{\pm} = \log [1 + 2e^{\beta_{\pm}} \cosh \beta_c]$. The average of an observable $o(\mathbf{s})$ with respect to the measure (S7) is given by

$$\langle o \rangle = \sum_{\mathbf{s}} \mathbb{P}(\mathbf{s}) o(\mathbf{s}). \quad (\text{S17})$$

Chemical potentials of the exponential measure (S9) are related to parameters of (S8) by matching averages

$$L^{-1} \langle Q_{\pm} \rangle = \partial_{\beta_{\pm}} f_{\text{eq}} = \rho_{\pm}/2, \quad L^{-1} \langle Q_c \rangle = \partial_{\beta_c} f_{\text{eq}} = (\rho_- + \rho_+)b/2, \quad (\text{S18})$$

which gives the identification

$$\beta_{\pm} = \log \left[\frac{\rho_{\pm} \sqrt{1-b^2}}{2\bar{\rho}_{\pm}} \right], \quad \beta_c = \frac{1}{2} \log \left[\frac{1+b}{1-b} \right], \quad (\text{S19})$$

with the inverses

$$\rho_{\pm} = \frac{\cosh \beta_c}{\cosh \beta_c + e^{-\beta_{\pm}}/2}, \quad b = \tanh \beta_c. \quad (\text{S20})$$

The static susceptibility is given by second derivatives of the free energy

$$C_{ii'} = \partial_{\beta_i} \partial_{\beta_{i'}} f_{\text{eq}} = L^{-1} \sum_{x,x'=1}^L \langle \hat{q}_{x,t}^i \hat{q}_{x',t}^{i'} \rangle^c, \quad (\text{S21})$$

where $\langle xy \rangle^c \equiv \langle xy \rangle - \langle x \rangle \langle y \rangle$. A simple direct calculation now gives the susceptibility matrix

$$C = \begin{bmatrix} C_{++} & C_{+-} & C_{+c} \\ C_{-+} & C_{--} & C_{-c} \\ C_{c+} & C_{c-} & C_{cc} \end{bmatrix} = \frac{1}{2} \begin{bmatrix} \rho_+ \bar{\rho}_+ & 0 & b\rho_+ \bar{\rho}_+ \\ 0 & \rho_- \bar{\rho}_- & b\rho_- \bar{\rho}_- \\ b\rho_+ \bar{\rho}_+ & b\rho_- \bar{\rho}_- & 2\rho(1 - 2b^2 p) \end{bmatrix}, \quad (\text{S22})$$

where $\rho \equiv (\rho_+ + \rho_-)/2$ and $p \equiv (\rho_+ - \rho_-)/2$ are the average particle and momentum density per lattice site. We now consider the static charge-current correlator

$$B_{ii'} = L^{-1} \sum_{x,x'=1}^L \langle \hat{q}_{x,t}^i \hat{j}_{x',t+1}^{i'} \rangle^c. \quad (\text{S23})$$

Left/right movers move freely along diagonals of distinct sublattices with velocities ± 1 which together with the symmetry $B_{ii'} = B_{i'i}$ immediately gives

$$B_{\pm\mp} = 0, \quad B_{\pm\pm} = \pm \rho_{\pm} \bar{\rho}_{\pm} / 2, \quad B_{\pm c} = B_{c\pm} = \pm \rho_{\pm} \bar{\rho}_{\pm} b / 2. \quad (\text{S24})$$

It only remains to evaluate the B_{cc} element, which is facilitated by noting that the local dynamics (S2) generate a non-zero charge current only in the following six configurations

$$(\emptyset, \pm) \leftrightarrow (\pm, \emptyset), \quad (+, -) \leftrightarrow (-, +). \quad (\text{S25})$$

However, the latter two configurations enter into the average (S23) with identical ensemble weights while their current values are oppositely signed so that their contributions identically cancel. This also shows that B is independent of the crossing parameter Γ . Evaluating the remaining non-zero charge current configurations we find

$$B_{cc} = p(1 - 2b^2 \rho). \quad (\text{S26})$$

which gives the full static charge-current correlator

$$B = \begin{bmatrix} B_{++} & B_{+-} & B_{+c} \\ B_{-+} & B_{--} & B_{-c} \\ B_{c+} & B_{c-} & B_{cc} \end{bmatrix} = \frac{1}{2} \begin{bmatrix} \rho_+ \bar{\rho}_+ & 0 & \rho_+ \bar{\rho}_+ b \\ 0 & -\rho_- \bar{\rho}_- & -\rho_- \bar{\rho}_- b \\ \rho_+ \bar{\rho}_+ b & -\rho_- \bar{\rho}_- b & 2p(1 - 2b^2 \rho) \end{bmatrix}. \quad (\text{S27})$$

Knowing the static susceptibilities, we get the flux Jacobian by inverting the relation $B = AC$ which yields

$$A = BC^{-1} = \begin{bmatrix} 1 & 0 & 0 \\ 0 & -1 & 0 \\ b\rho_-/\rho & -b\rho_+/\rho & v \end{bmatrix}, \quad (\text{S28})$$

where $v \equiv (\rho_+ - \rho_-)/(\rho_+ + \rho_-) = p/\rho$. With this, we obtain the closed three-component Euler hydrodynamic equations

$$\begin{cases} \partial_t \frac{\rho^\pm}{2} \pm \partial_x \frac{\rho^\pm}{2} = 0 \\ \partial_t \rho_c + \partial_x (v \rho_c) = 0 \end{cases}. \quad (\text{S29})$$

Note that a closure of the hydrodynamic hierarchy within a subset of conserved charges also happens in other cellular automata, e.g. the Rule 54 [1]. Diagonalizing the flux Jacobian as $RAR^{-1} = \text{diag}(1, -1, v)$, its sign readily follows

$$\text{sgn } A \equiv R^{-1} \text{sgn}[\text{diag}(1, -1, v)]R = \begin{bmatrix} 1 & 0 & 0 \\ 0 & -1 & 0 \\ 2b\Theta(-p) & -2b\Theta(p) & \text{sgn } p \end{bmatrix}, \quad (\text{S30})$$

where Θ is the Heaviside step function.

III. BALLISTIC MACROSCOPIC FLUCTUATION THEORY SOLUTION

The dynamic equations of ballistic macroscopic fluctuation theory at fixed counting field λ read

$$\partial_t \beta^\pm(x, t) \pm \partial_x \beta^\pm(x, t) \pm b(x, t) \frac{\varrho_\mp(x, t)}{\varrho(x, t)} \partial_x \beta^c(x, t) = 0, \quad (\text{S31})$$

$$\partial_t H^\pm(x, t) \pm \partial_x H^\pm(x, t) \pm b(x, t) \frac{\varrho_\mp(x, t)}{\varrho(x, t)} \partial_x H^c(x, t) = 0, \quad (\text{S32})$$

$$\partial_t \beta^c(x, t) + v(x, t) \partial_x \beta^c(x, t) = 0, \quad (\text{S33})$$

$$\partial_t H^c(x, t) + v(x, t) \partial_x H^c(x, t) = 0, \quad (\text{S34})$$

The dynamic equations are supplemented with boundary condition at $t = 0$ and $t = \tau$

$$H^\pm(x, 0) = \beta^\pm(x, 0) - \beta^\pm, \quad (\text{S35})$$

$$H^\pm(x, 1) = 0, \quad (\text{S36})$$

$$H^c(x, 0) = \beta^c(x, 0) - \beta^c + \lambda \Theta(x), \quad (\text{S37})$$

$$H^c(x, 1) = \lambda \Theta(x). \quad (\text{S38})$$

We now consider the system of dynamical equation by using the method of characteristics, starting with the pair of charge equations (S33) and (S34), whose characteristic $x(t)$ are given implicitly by

$$\frac{d}{dt} x = v(x(t), t). \quad (\text{S39})$$

The fields $\beta^c(x, t)$ and $H^c(x, t)$ are constant along the charge characteristics $x(t)$

$$\frac{d}{dt}\beta^c(x(t), t) = \frac{d}{dt}H^c(x(t), t) = 0. \quad (\text{S40})$$

We introduce two charge characteristics distinguished by their boundary points at $t = 0$ and $t = 1$

$$x_1(t) = \left\{ \frac{d}{dt}x_1 = v(x_1(t), t) \mid x_1(0) = 0 \right\}, \quad x_2(t) = \left\{ \frac{d}{dt}x_2 = v(x_2(t), t) \mid x_2(1) = 0 \right\}. \quad (\text{S41})$$

For later convenience we note that

$$\text{sgn } v = \text{sgn}(\rho_+ - \rho_-) = \text{sgn}(e^{\beta^+} - e^{\beta^-}) = \text{sgn}(\beta^+ - \beta^-). \quad (\text{S42})$$

Evolving the boundary condition for $H^c(x, \tau)$ (S38) backwards in time we have

$$H^c(x, t) = \lambda\Theta(x - x_2(t)). \quad (\text{S43})$$

The boundary condition $H^c(x, 0)$ (S37) now gives

$$\beta^c(x, 0) = \beta^c + \lambda [\Theta(x - x_2(t)) - \Theta(x)]. \quad (\text{S44})$$

Since $\beta^c(x, t)$ is constant along charge characteristic we can evolve it forwards in time to find

$$\beta^c(x, t) = \beta^c + \lambda [\Theta(x - x_2(t)) - \Theta(x - x_1(t))]. \quad (\text{S45})$$

We now turn to the equations for left/right movers, whose characteristics $x_{\pm}(t)$ are trivial

$$x_{\pm}(t) = x \pm t \quad (\text{S46})$$

along which the fields $H^{\pm}(x, t)$ evolve according to

$$\frac{d}{dt}H^{\pm}(x_{\pm}(x, t), t) = \mp \lambda b(x_{\pm}(t), t) \frac{\varrho_{\mp}(x_{\pm}(t), t)}{\varrho(x_{\pm}(t), t)} \delta(x_{\pm}(t) - x_2(t)). \quad (\text{S47})$$

We now observe that

$$\frac{\varrho_{\mp}(x_{\pm}(t), t)}{\varrho(x_{\pm}(t), t)} \delta(x_{\pm}(t) - x_i(t)) = \delta(t - t_i), \quad (\text{S48})$$

where t_i is the time at which (if any), the characteristic x_{\pm} cross x_i , $x_{\pm}(t_i) = x_i(t_i)$. Using (S48) and (S47) we integrate the boundary conditions $H^{\pm}(x, \tau)$ backwards along the $x_{\pm}(t)$ characteristics to find

$$H^{\pm}(x, t) = \lambda b_2 [\Theta(x_2(t) - x) - \Theta(\mp(\tau - t) - x)], \quad (\text{S49})$$

where we noted that $b(x_i(t), t) = b_i$ is constant along $x_i(t)$. We emphasize that b_2 cannot be identified with $\tanh \beta^c(0, \tau)$, the value of β^c at that point being singular due to the incidence of

the contour x_2 . However, the solution (S49) shows that $H^\pm(x, 0)$ are constant on the intervals $(-1, x_2(0))$ and $(x_2(0), 1)$ respectively. To determine its value, we note that the pair of Eqs. (S32) can be rewritten as

$$\frac{d}{dt} [H^\pm(x_\pm(t), t) + \log \cosh \beta^c(x_\pm(t), t)] = \mp \lambda b_1 \delta(t - t_1). \quad (\text{S50})$$

We now use (S50) to propagate the initial condition (S36) from $t = 1$ back to $t = 0$ along trajectories that do not cross x_1 , which, together with (S49) allows us to fully specify $H^\pm(x, 0)$

$$H_\pm(x, 0) = s [\Theta(x_2(t) - x) - \Theta(\mp(1 - t) - x)] \log \left[\frac{\cosh \beta^c(\lambda)}{\cosh \beta^c} \right], \quad (\text{S51})$$

where $\beta^c(\lambda) = \beta^c + \lambda s$ and $s = \text{sgn}(x_1 - x_2)$. We have suppressed the time dependence of the sign which is constant as will be demonstrated shortly. From the boundary condition (S35) we now read off

$$\beta^\pm(x, 0) = \beta^\pm + s [\Theta(x_2(t) - x) - \Theta(\mp(1 - t) - x)] \log \left[\frac{\cosh \beta^c(\lambda)}{\cosh \beta^c} \right]. \quad (\text{S52})$$

We now note that the pair of Eqs. (S31) can be rewritten as

$$\frac{d}{dt} [\beta^\pm(x_\pm(t), t) + \log \cosh \beta^c(x_\pm(t), t)] = 0, \quad (\text{S53})$$

so that $\beta^\pm + \log \cosh \beta^c$ is constant along the characteristics x_\pm . Combined with (S52) this gives the solution

$$\beta^+(x, t) = \beta^+ + s [\Theta(t - x) - \Theta(-1 + t - x) - \Theta(x_1(t) - x) + \Theta(x_2(t) - x)] \log \left[\frac{\cosh \beta^c(\lambda)}{\cosh \beta^c} \right], \quad (\text{S54})$$

$$\beta^-(x, t) = \beta^- - s [\Theta(1 - t - x) - \Theta(-t - x) + \Theta(x_1(t) - x) - \Theta(x_2(t) - x)] \log \left[\frac{\cosh \beta^c(\lambda)}{\cosh \beta^c} \right]. \quad (\text{S55})$$

Specializing to $x = 0$ we find

$$\beta^\pm(0, t) = \beta^\pm - 2\Theta(\mp s) \log \left[\frac{\cosh \beta^c(\lambda)}{\cosh \beta^c} \right]. \quad (\text{S56})$$

It remains to establish the sign s and show that it is independent of time. From Eqs. (S54) and (S55) we find that the velocities along the characteristics x_1 and x_2 are constant and equal to each other inside the square spanned by the points $(-1/2, 1/2)$, $(0, 1)$, $(1/2, 1/2)$ and $(0, 0)$. Outside of this square the trajectory velocities change to different constant values. However, since $x_1(t)$ and $x_2(t)$ begin and terminate at $x = 0$ respectively, and the magnitudes of velocities are bounded by

one they cannot cross the line $x = 0$ again and their signs are therefore constant in time. The sign values are most easily obtained by considering the signs of velocities at $x_1(0) = 0$ and at $x_2(1) = 0$, where we find

$$\beta^+(0, 0) - \beta^-(0, 0) = \beta^+(0, 1) - \beta^-(0, 1) = \beta^+ - \beta^- + s \log \left[\frac{\cosh(\beta^c(\lambda))}{\cosh \beta^c} \right]. \quad (\text{S57})$$

Noting that x_1 and x_2 have constant and opposite signs we now have

$$s = \text{sgn}(x_1 - x_2) = \text{sgn}(x_1) = -\text{sgn}(x_2) = \text{sgn} \left(\beta_+ - \beta_- + s \log \left[\frac{\cosh(\beta_c(\lambda))}{\cosh \beta_c} \right] \right). \quad (\text{S58})$$

For simplicity we now specialize to $\beta^\pm = \beta$, where

$$s = s \text{sgn} \left(\log \left[\frac{\cosh(\beta^c + \lambda s)}{\cosh \beta^c} \right] \right) = s^2 \text{sgn}(\lambda \beta^c) = \text{sgn}(\lambda b). \quad (\text{S59})$$

The solution along the central ray $x = 0$ is time-independent and for $\beta_\pm = \beta$ finally reads

$$\beta^c(0, t) = \beta^c(\lambda) = \beta^c + |\lambda| \text{sgn } b, \quad (\text{S60})$$

$$\beta^\pm(0, t) = \beta^\pm(\lambda) = \beta - 2 \log \left[\frac{\cosh(\beta^c + |\lambda| \text{sgn } b)}{\cosh \beta^c} \right] \Theta(\mp \lambda b). \quad (\text{S61})$$

Using the relations (S20) we now find after some algebra

$$b(\lambda) = s \partial_\lambda \log \mu_b, \quad (\text{S62})$$

$$\rho_\pm(\lambda) = \frac{\rho}{\rho + (1 - \rho) \mu_b^{\mp s}}, \quad (\text{S63})$$

where $\mu_b = \cosh \lambda + |b| \sinh |\lambda|$ and $\rho = \frac{\cosh \beta^c}{\cosh \beta^c + e^{-\beta/2}}$. The charge scaled cumulant generating function (SCGF) is now given by

$$F(\lambda) = \int_0^\lambda d\lambda' j_c(\lambda') = \frac{1}{2} \int_0^\lambda d\lambda' [\rho_+(\lambda') - \rho_-(\lambda')] b(\lambda') = \frac{1}{2} \int_0^\lambda d\lambda' s' \frac{\Delta^2 (\mu_b^{s'} - \mu_b^{-s'}) \partial_{\lambda'} \log \mu_b}{1 + \Delta^2 (\mu_b + \mu_b^{-1} - 2)} \quad (\text{S64})$$

$$= \frac{1}{2} \log [1 + \Delta^2 (\mu_b + \mu_b^{-1} - 2)], \quad \Delta^2 = \rho(1 - \rho), \quad (\text{S65})$$

which reproduces the exact microscopic result of Ref. [2] up to a prefactor of 1/2 which stems from a rescaling of time by a factor of two compared to the present work.

IV. COMPARISON BETWEEN BMFT AND BFT

It was argued in Ref. [3] that BMFT in fact reduces to ballistic fluctuation theory (BFT) [4–6] when the former was specialized to equilibrium. Let us demonstrate that this is indeed the case in

the SCCA as well. BFT is a large deviation theory that describes the current fluctuations of the system that supports ballistic transport. A major difference between BFT and BMFT is that BFT is applicable only to systems in equilibrium, which makes the structure of BFT easier to handle. The main observation in BFT is that the insertion of the operator $e^{\lambda J(t)}$ in a GGE amounts to a modification of the GGE parameterized by the Lagrange multipliers $\underline{\beta}$ into that parameterized by the λ -dependent Lagrange multipliers $\underline{\beta}(\lambda)$. Adopting to the charge transport in the SCCA, such multipliers $\underline{\beta}(\lambda)$ turn out to satisfy the so-called flow equation

$$\partial_\lambda \beta^i(\lambda) = [\text{sgn} \mathbf{A}(\lambda)]_c^i, \quad (\text{S66})$$

where $\mathbf{A}(\lambda)$ is the flux Jacobian evaluated with respect to the multipliers $\underline{\beta}(\lambda)$. More explicitly, the equations for multipliers read

$$\partial_\lambda \beta^\pm(\lambda) = \pm 2b \Theta(\mp(\beta^+(\lambda) - \beta^-(\lambda))), \quad \partial_\lambda \beta^c(\lambda) = \text{sgn}(\beta^+(\lambda) - \beta^-(\lambda)). \quad (\text{S67})$$

In terms of the solution of the flow equation, the SCGF is given by

$$F(\lambda) = \int_0^\lambda d\lambda' j_c(\lambda'), \quad (\text{S68})$$

where $j_c(\lambda)$ is the charge current evaluated again with respect to $\underline{\beta}(\lambda)$. The flow equation Eq. (S67) can be in fact solved explicitly (for $\beta^\pm = \beta$) as

$$\beta^c(\lambda) = \beta^c + \text{sgn } b |\lambda|, \quad (\text{S69})$$

$$\beta^\pm(\lambda) = \beta - 2\Theta(\mp \lambda b) \log \left[\frac{\cosh(\beta^c + |\lambda| \text{sgn } b)}{\cosh \beta^c} \right], \quad (\text{S70})$$

which precisely coincide with the solution of the BMFT equations at $x = 0$ Eqs. (S60) and (S61). We thus confirm that the modified λ -dependent GGE is indeed realized along the ray $x = 0$ as proposed in Ref. [3].

V. CHARGE-CHARGE TRANSPORT COEFFICIENT

As a check of the hydrodynamic framework we compare its of the charge transport coefficients against those obtained from exact microscopic calculations. The microscopic input is the unequal-time charge current correlation

$$F_{cc}(t) = L^{-1} \sum_{x,x'=1}^L \langle \hat{j}_{x,1/2}^c \hat{j}_{x,t+1/2}^c \rangle^c, \quad (\text{S71})$$

which has been computed exactly in [7] which uses a somewhat different parametrization compared to that employed in this work. The identification is made by substituting

$$\rho \rightarrow \frac{\rho_+ + \rho_-}{2} = \rho, \quad \Delta \rightarrow \frac{\rho_+ - \rho_-}{2} = p, \quad \mu \rightarrow b \frac{\rho_+ + \rho_-}{2} = b\rho, \quad (\text{S72})$$

and identifying the time and charge currents as

$$t \rightarrow 2t, \quad j^c \rightarrow \hat{j}^c/4. \quad (\text{S73})$$

For $\Gamma = 0$ the dynamics is deterministic and the Drude weight and Onsager coefficient are given by a pair of discrete-time Green-Kubo relations

$$\mathcal{D}_{cc} = \lim_{t \rightarrow \infty} t^{-1} \sum_{t'=0}^t {}'F_{cc}(t'), \quad \mathcal{L}_{cc} = \sum_{t=0}^{\infty} {}'(F_{cc}(t) - \mathcal{D}_{cc}). \quad (\text{S74})$$

where we regularize the sums as $\sum_{j=0}^{\infty} {}'f(t) = \frac{1}{2}f(0) + \sum_{t=1}^{\infty} f(t)$.

A. Microscopic result

The expression for the charge current correlation (S71) in Equation 3.18 of Ref. [7] contains a typo [8]. The correct expression reads

$$F_{cc}(t=0) = 8\bar{\rho}[\mu^2 + \rho(2-\rho)] + 8\Delta^2(3-\rho-\mu^2(5-\rho)/\rho^2), \quad (\text{S75})$$

$$F_{cc}(t \geq 1) = 16\rho \left[(1-\rho)\mu^2/\rho^2 + \Delta^2/\rho^2(1 - (1+\rho)\mu^2/\rho^2) \right] + \quad (\text{S76})$$

$$16\rho(1-\rho)^4(1-\mu^2/\rho^2)(1-\Delta^2/\rho^2)(1-2\rho)^{2t-2}, \quad (\text{S77})$$

which after the substitutions (S72), (S73) and computing the sums (S74) gives

$$\mathcal{D}_{cc} = \rho\bar{\rho}b^2 + 16\rho v^2(1-b^2(1+\rho)), \quad (\text{S78})$$

$$\mathcal{L}_{cc} = \frac{1}{2}\bar{\rho}(1-v^2)(1-b^2). \quad (\text{S79})$$

B. Hydrodynamic result

In Ref. [9], a lower bound of the Onsager coefficient \mathcal{L}_{cc}

$$\mathcal{L}_{ij} \geq \mathcal{L}_{ij}^{\text{LB}} = (R^{-1}\tilde{G}^2R^{-\text{T}})_{cc} \quad (\text{S80})$$

was derived, where R is the matrix that diagonalizes A as $RAR^{-1} = \text{diag } \underline{v}^{\text{eff}}$, and

$$\tilde{G}_{ij}^2 = \sum_{k,l=1,2,3} \frac{G_i^{kl}G_{jkl}}{|v_k^{\text{eff}} - v_l^{\text{eff}}|}, \quad \underline{v}^{\text{eff}} = (1-1, v) \quad (\text{S81})$$

Here the G -tensor $G_i^{jk} = R_i^l (R^{-T} H_l R^{-1})^{jk}$ is given by the Hessian $H_i^{jk} = \partial A_i^j / \partial \rho_k$. The bound is known to be saturated in integrable systems [9]. Since the SCCA is super-integrable, we expect that the lower bound also gives the exact Onsager coefficient. We first observe that the Hessian H_i^{jk} is nontrivial only when $i = 3$, and we have

$$H_3 = \frac{1}{\rho^2} \begin{pmatrix} -2b\rho_- & b(\rho_+ - \rho_-) & \rho_- \\ b(\rho_+ - \rho_-) & 2b\rho_+ & -\rho_+ \\ \rho_- & -\rho_+ & 0 \end{pmatrix}, \quad (\text{S82})$$

which also indicates that G_3^{ij} are also the only nontrivial entries in G . As a result, the convective Onsager matrix is nontrivial only for \mathcal{L}_{33}^c as well. Normalizing R by requiring $RCR^T = I$, where I is the identity matrix, R is explicitly given by

$$R = \begin{pmatrix} \frac{1}{\sqrt{\rho_+(1-\rho_+)}/2} & 0 & 0 \\ 0 & \frac{1}{\sqrt{\rho_-(1-\rho_-)}/2} & 0 \\ -\frac{b}{\sqrt{(1-b^2)\rho}} & -\frac{b}{\sqrt{(1-b^2)\rho}} & \frac{1}{\sqrt{(1-b^2)\rho}} \end{pmatrix}, \quad (\text{S83})$$

which allows us to compute \tilde{G}_{33}^2 as

$$\tilde{G}_{33}^2 = \frac{\rho_+\rho_-(2 - \rho_+ - \rho_-)}{4\rho^3}. \quad (\text{S84})$$

Plugging this into (S80), we are finally in the position to compute $\mathcal{L}_{cc}^{\text{LB}}$, which reads

$$\mathcal{L}_{cc}^{\text{LB}} = \frac{(1-b^2)\rho_+\rho_-(2 - \rho_+ - \rho_-)}{4\rho^2}. \quad (\text{S85})$$

This reproduces the microscopic result Eq. (S79) as expected.

VI. TYPICAL CHARGE FLUCTUATIONS

In this Section we quantify fluctuations of the time-integrated charge current

$$\hat{J}(t) = \sum_{t'=0}^t \hat{j}_{0,t'+1/2}^c. \quad (\text{S86})$$

The scale of typical fluctuations is set by the variance of the integrated current

$$\left\langle \left[\hat{J}(t) \right]^2 \right\rangle^c \sim t^{1/z}, \quad (\text{S87})$$

where z is the dynamical exponent. We specialize to maximum entropy ensembles with no average charge or momentum which correspond to $\rho_{\pm} = \rho$, $p = 0$ and $b = 0$, where the dynamical exponent

is diffusive, $z = 2$. Finite-time distribution of fluctuations of the integrated charge current on the typical scale converge asymptotically to the typical distribution

$$\mathcal{P}_{\text{typ}}^{[\Gamma]}(j) = \lim_{t \rightarrow \infty} t^{1/2z} \mathcal{P}^{[\Gamma]}(J = jt^{1/2z}|t). \quad (\text{S88})$$

The typical distribution in the deterministic single-file limit ($\Gamma = 0$) has been derived in [2]. Here we reproduce it based on the idea inspired by BMFT.

A. Typical fluctuations at $b \neq 0$

As explained in the main text, the main assumption here is that, in the single-file case, the typical fluctuations are fully characterized by the initial typical fluctuations that are propagated in time by the Euler equation. The initial typical fluctuations are prescribed by the fluctuating fields $\varrho_i(x, 0) = \hat{\varrho}_i(\tau x, 0)$

$$\varrho_i(x, 0) \simeq \rho_i + \tau^{-1/2} \delta\varrho_i(x, 0), \quad (\text{S89})$$

where ρ_i is the background density and the deviation $\delta\varrho_i(x, 0)$ is Gaussian-distributed with $\langle \delta\varrho_i(x, 0) \delta\varrho_j(y, 0) \rangle = C_{ij} \delta(x - y)$. Since such fluctuations are disseminated by the Euler equation, the left and right movers remain diffusively fluctuate

$$\delta\varrho_{\pm}(x, t) \simeq \rho + \tau^{-1/2} \delta\varrho_{\pm}(x \mp t, 0). \quad (\text{S90})$$

We thus realize that the Euler-scale charge current $j_c(0, t)$ has the leading behavior

$$\begin{aligned} j_c(0, t) &= b(0, t) \frac{\varrho_+(0, t) - \varrho_-(0, t)}{2} \\ &\simeq b\tau^{-1/2} \frac{\delta\varrho_+(0, t) - \delta\varrho_-(0, t)}{2} \simeq b\tau^{-1/2} \frac{\delta\varrho_+(-t, 0) - \delta\varrho_-(t, 0)}{2}. \end{aligned} \quad (\text{S91})$$

Note that the fluctuation of the normal mode $b(x, t)$ does not contribute here. With these, we can write down the cumulant generating function as a Gaussian integral

$$\langle e^{\lambda \hat{J}_c(\tau)} \rangle \simeq \frac{1}{Z} \int_{(\mathbb{R})} \mathcal{D}\underline{\delta\varrho}(\cdot, 0) e^{-\frac{C_{ij}}{2} \int_{\mathbb{R}} dx \delta\varrho_i(x, 0) \delta\varrho_j(x, 0)} e^{\frac{b\lambda\sqrt{\tau}}{2} \int_0^1 dt (\delta\varrho_+(-t, 0) - \delta\varrho_-(t, 0))} \quad (\text{S92})$$

To compute the normalization factor Z , we recast the integral in terms of the normal mode $\delta\varrho = R^{-1} \delta n$ such that $RCR^T = I$. The inverse of such a transformation matrix R Eq. (S83) reads explicitly

$$R^{-1} = \frac{1}{\sqrt{2}} \begin{pmatrix} \sqrt{\rho_+(1 - \rho_+)} & 0 & 0 \\ 0 & \sqrt{\rho_-(1 - \rho_-)} & 0 \\ b\sqrt{\rho_+(1 - \rho_+)} & b\sqrt{\rho_-(1 - \rho_-)} & \sqrt{(1 - b^2)(\rho_+ + \rho_-)} \end{pmatrix}, \quad (\text{S93})$$

which gives

$$Z \simeq \int_{(\mathbb{R})} \mathcal{D}\underline{\varrho}(\cdot, 0) e^{-\frac{c_{ij}}{2} \int_{\mathbb{R}} dx \delta \varrho_i(x, 0) \delta \varrho_j(x, 0)} = (2\pi)^{3/2} \det R^{-1} = \sqrt{2\pi(1-b^2)} \rho \Delta^2. \quad (\text{S94})$$

With this we can evaluate the functional integral as

$$\langle e^{\lambda \hat{J}_c(\tau)} \rangle \simeq \frac{1}{2\pi} \int_{(\mathbb{R})} \mathcal{D}\underline{n}(\cdot, 0) e^{-\int_{\mathbb{R}} dx [\frac{1}{2}(\delta n_i(x, 0))^2 - \mu_1(x) \delta n_1(x, 0) - \mu_2(x) \delta n_2(x, 0)]} \quad (\text{S95})$$

where

$$\mu_1(x) = \frac{\lambda b \sqrt{\tau} \Delta}{\sqrt{2}} \chi(-1 < x < 0), \quad \mu_2(x) = -\frac{\lambda b \sqrt{\tau} \Delta}{\sqrt{2}} \chi(0 < x < 1), \quad (\text{S96})$$

with $\chi(x)$ the indicator function. Performing the integral explicitly, we finally get

$$\langle e^{\lambda \hat{J}(\tau)} \rangle \simeq e^{\frac{\tau \lambda^2 \sigma^2}{2}}, \quad \sigma^2 = (b\Delta)^2. \quad (\text{S97})$$

Transforming back to the probability distribution $\mathcal{P}(j\tau^{-1/2z}|\tau) = (2\pi)^{-1} \int_{\mathbb{R}} d\lambda e^{-i\lambda j\tau^{1/2z}} \langle e^{i\lambda \hat{J}(\tau)} \rangle$, we finally get

$$\mathcal{P}_{\text{typ}}^{[0]}(j) = \frac{1}{\sqrt{2\pi\sigma^2}} e^{-\frac{j^2}{2\sigma^2}}. \quad (\text{S98})$$

B. Typical fluctuations at $b = 0$

The situation at half-filling $b = 0$ calls for a separate treatment as the dynamical exponent in this case is $z = 2$. In this case the appropriate scale to work with is the diffusive scale where the space-time coordinate (x, t) is rescaled as $(\sqrt{\tau}x, \tau t)$. Accordingly we define the fluctuating density fields at the diffusive scale as $\varrho(x, t) = \hat{\varrho}(\sqrt{\tau}x, \tau t)$. At this scale the left and right movers initially fluctuate as

$$\varrho_{\pm}(x, 0) = \rho + \tau^{-1/4} \delta \varrho_{\pm}(x, 0) \quad (\text{S99})$$

and still follow the Euler equation $\partial_t \varrho_{\pm}(x, t) \pm \sqrt{\tau} \partial_x \varrho_{\pm}(x, t) = 0$ with the solution

$$\varrho_{\pm}(x, t) = \rho + \tau^{-1/4} \delta \varrho_{\pm}(x \mp \sqrt{\tau}t, 0). \quad (\text{S100})$$

Likewise, the charge density also fluctuates around zero at half-filling as

$$\varrho_c(x, t) = \tau^{-1/4} \delta \varrho_c(x, 0) \quad (\text{S101})$$

and the field $b(x, t)$ satisfies the equation $\partial_t b(x, t) + \sqrt{\tau} v(x, t) \partial_x b(x, t) = 0$. The solution is then

$$b(x, t) = b(x - X_d(t), 0) \simeq \frac{\tau^{-1/4}}{\rho} \delta \varrho_c(x - X_d(t), 0), \quad (\text{S102})$$

where the characteristic line $X_d(t)$ satisfies

$$\begin{aligned} \frac{dX_d(t)}{dt} &= \tau^{1/4} \frac{\delta \varrho_+(X_d(t) - \sqrt{\tau}t, 0) - \delta \varrho_-(X_d(t) + \sqrt{\tau}t, 0)}{2\rho + T^{-1/4}(\delta \varrho_+(X_d(t) - \sqrt{\tau}t, 0) + \delta \varrho_-(X_d(t) + \sqrt{\tau}t, 0))} \\ &\simeq \tau^{1/4} \frac{\delta \varrho_+(-\sqrt{\tau}t, 0) - \delta \varrho_-(\sqrt{\tau}t, 0)}{2\rho}. \end{aligned} \quad (\text{S103})$$

Note that in the last line we used the fact that $X_d(t)$ fluctuates on the scale $\tau^{1/4}$. With these, we can now evaluate the charge current at the diffusive scale $j_{d,c}(0, t) = \sqrt{\tau} \hat{j}(0, \tau t)$ as

$$\begin{aligned} j_{d,c}(0, t) &\simeq \frac{\delta \varrho_c(-X_d(t), 0)}{2\rho} (\delta \varrho_+(-\sqrt{\tau}t, 0) - \delta \varrho_-(\sqrt{\tau}t, 0)) \\ &= \tau^{-1/4} \partial_t \int_0^{X_d(t)} dx \delta \varrho_c(-x, 0). \end{aligned} \quad (\text{S104})$$

Therefore, the time-integrated current in terms of the diffusive current reads

$$\hat{J}_c(\tau) = \int_0^\tau dt \hat{j}(0, t) = \sqrt{\tau} \int_0^1 dt j_{d,c}(0, t) = \tau^{1/4} \int_0^{X_d(1)} dx \delta \varrho_c(-x, 0). \quad (\text{S105})$$

Plugging this into the path-integral, we then have

$$\langle e^{\lambda \hat{J}_c(\tau)} \rangle \simeq \frac{1}{Z} \int_{(\mathbb{R})} \mathcal{D}\underline{\varrho}(\cdot, 0) e^{-\frac{c^{ij}}{2} \int_{\mathbb{R}} dx \delta \varrho_i(x, 0) \delta \varrho_j(x, 0)} e^{\lambda \tau^{1/4} \int_0^{X_d(1)} dx \delta \varrho_c(-x, 0)} \quad (\text{S106})$$

$$\begin{aligned} &= \frac{1}{(2\pi)^{3/2}} \int_{(\mathbb{R})} \mathcal{D}\underline{n}(\cdot, 0) e^{-\frac{1}{2} \int dx [(\delta n_i(x, 0))^2 - 2\lambda \tau^{1/4} \sqrt{\rho} \chi(-|X_d(1)| < x < 0) \delta n_c(x, 0)]} \\ &= \frac{1}{2\pi} \int_{(\mathbb{R})} \mathcal{D}\delta n_1(\cdot, 0) \mathcal{D}\delta n_2(\cdot, 0) e^{-\frac{1}{2} \int dx [(\delta n_1(x, 0))^2 + (\delta n_2(x, 0))^2 - \lambda^2 \tau^{1/2} \rho |X_d(1)|]}. \end{aligned} \quad (\text{S107})$$

Assuming $X_d(t)$ is monotonic in time and $\delta n_1(-x, 0) = \delta n_1(x, 0)$, we then have

$$\langle e^{\lambda \hat{J}_c(\tau)} \rangle \simeq \frac{1}{2\pi} \int_{(\mathbb{R})} \mathcal{D}\delta n_1(\cdot, 0) \mathcal{D}\delta n_2(\cdot, 0) e^{-\frac{1}{2} \int_{\mathbb{R}} dx [(\delta n_1(x, 0))^2 + (\delta n_2(x, 0))^2]} e^{\frac{\Delta \lambda^2 \tau^{1/4}}{2\sqrt{2}} \int_0^{\sqrt{\tau}} dx |\delta n_1(x, 0) - \delta n_2(x, 0)|}. \quad (\text{S108})$$

Introducing the variables $\delta n = (\delta n_1 + \delta n_2)/\sqrt{2}$ and $\delta \bar{n} = (\delta n_1 - \delta n_2)/\sqrt{2}$, this becomes

$$\begin{aligned} \langle e^{\lambda \hat{J}_c(\tau)} \rangle &\simeq \frac{1}{2\pi} \int_{(\mathbb{R})} \mathcal{D}\delta n(\cdot, 0) \mathcal{D}\delta \bar{n}(\cdot, 0) e^{-\frac{1}{2} \int_{\mathbb{R}} dx [(\delta n(x, 0))^2 + (\delta \bar{n}(x, 0))^2]} e^{\frac{\Delta \lambda^2 \tau^{1/4}}{2} \int_0^{\sqrt{\tau}} dx |\delta \bar{n}(x, 0)|} \\ &= \frac{1}{\sqrt{2\pi}} \int_{(\mathbb{R})} \mathcal{D}\delta \bar{n}(\cdot, 0) e^{-\frac{1}{2} \int_{\mathbb{R}} dx (\delta \bar{n}(x, 0))^2} e^{\frac{\Delta \lambda^2 \tau^{1/4}}{2} \int_0^{\sqrt{\tau}} dx |\delta \bar{n}(x, 0)|} \\ &= e^{\xi^4/2} (1 + \text{erf}(\xi^2/\sqrt{2})), \end{aligned} \quad (\text{S109})$$

where $\xi^2 = \Delta \lambda^2 \sqrt{\tau}/2$. This in turn gives a non-Gaussian typical distribution

$$\mathcal{P}_{\text{typ}}^{[0]}(j) = \frac{1}{2\pi \Delta} \int_{\mathbb{R}} \frac{du}{\sqrt{|u|}} e^{-\frac{u^2}{2\Delta^2} - \frac{j^2}{2|u|}}. \quad (\text{S110})$$

As we discussed in the main text, we can make sense of the markedly different behaviors in the two cases $b \neq 0$ and $b = 0$ by appreciating which fluctuating fields are responsible for the charge

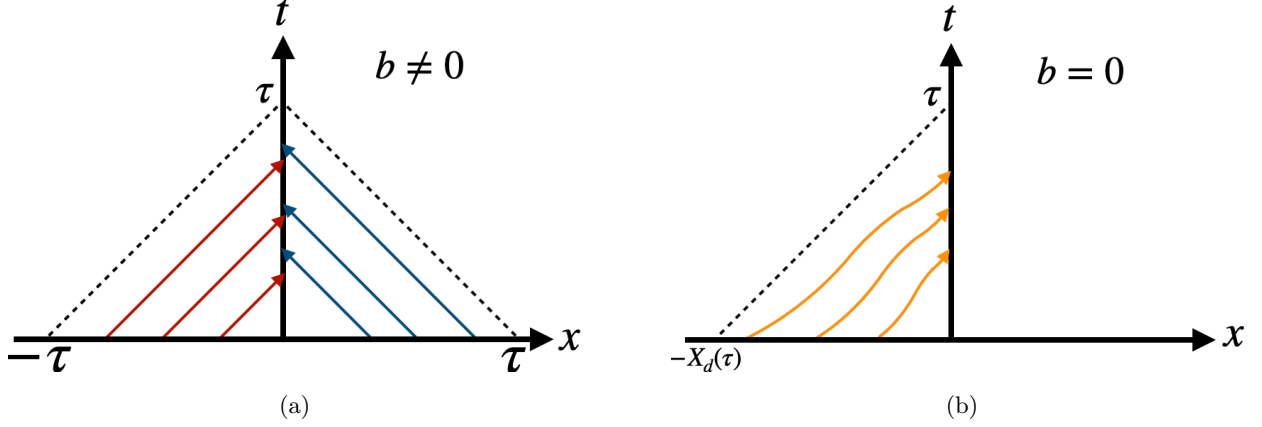


FIG. S1. Initial fluctuations that influence the charge current fluctuations. (a): when $b \neq 0$, the particle fluctuations $\delta\rho_{\pm}(x,0)$ that cross $x = 0$ between $t = 0$ and $t = \tau$ give rise to the current fluctuations. (b): when $b = 0$ the charge fluctuations $\delta\rho_c(x,0)$ that cross $x = 0$ between $t = 0$ and $t = \tau$ contribute to the current fluctuations. Note that while the trajectory is now nonlinear, the slope cannot exceed 1 because $|dX_d(t)/dt| < 1$. Here we assumed $X_d(t) > 0$ for $t \in [0, \tau]$.

current fluctuations. First, when $b \neq 0$, it can be readily seen in Eq. (S92) that the charge current fluctuations are completely determined by the initial particle fluctuations $\delta\rho_{\pm}$. Since particle fluctuations are propagated freely in time (see Fig. S1a), the initial Gaussian fluctuations remain intact and as a result the typical fluctuations keep Gaussianity. This is in stark contrast to what happens at half-filling where the current fluctuations are now given solely by the charge fluctuations that are transported nonlinearly with the velocity v as per Eq. (S106) (see Fig. S1b). Gaussianity is therefore not preserved during the dynamics, resulting in the non-Gaussian distribution.

C. Typical fluctuations in the stochastic case $\Gamma \neq 0$

Note that the distribution Eq. (S110) features a cusp at the origin. Numerical simulations for $\Gamma > 0$ indicate that the cusp is rounded off with stochastic crossings while the distribution remains non-Gaussian. This motivates a generalization of the single-file distribution (S110) of the form

$$\mathcal{P}_{\text{typ}}^{[\Gamma]}(j) = \int_{-\infty}^{\infty} \frac{du}{2\pi\sigma\sqrt{u^2 + \omega^2}} \exp\left[-\frac{u^2}{2\sigma^2} - \frac{j^2}{2\sqrt{u^2 + \omega^2}}\right], \quad (\text{S111})$$

which reduces to (S110) as $\omega \rightarrow 0$. Treating ω and σ as Γ -dependent fitting parameters, the distribution (S111) accurately captures the asymptotic typical distribution for $\Gamma \geq 0$ across 5 order of magnitude, as shown in Figure S2 and Table S1.

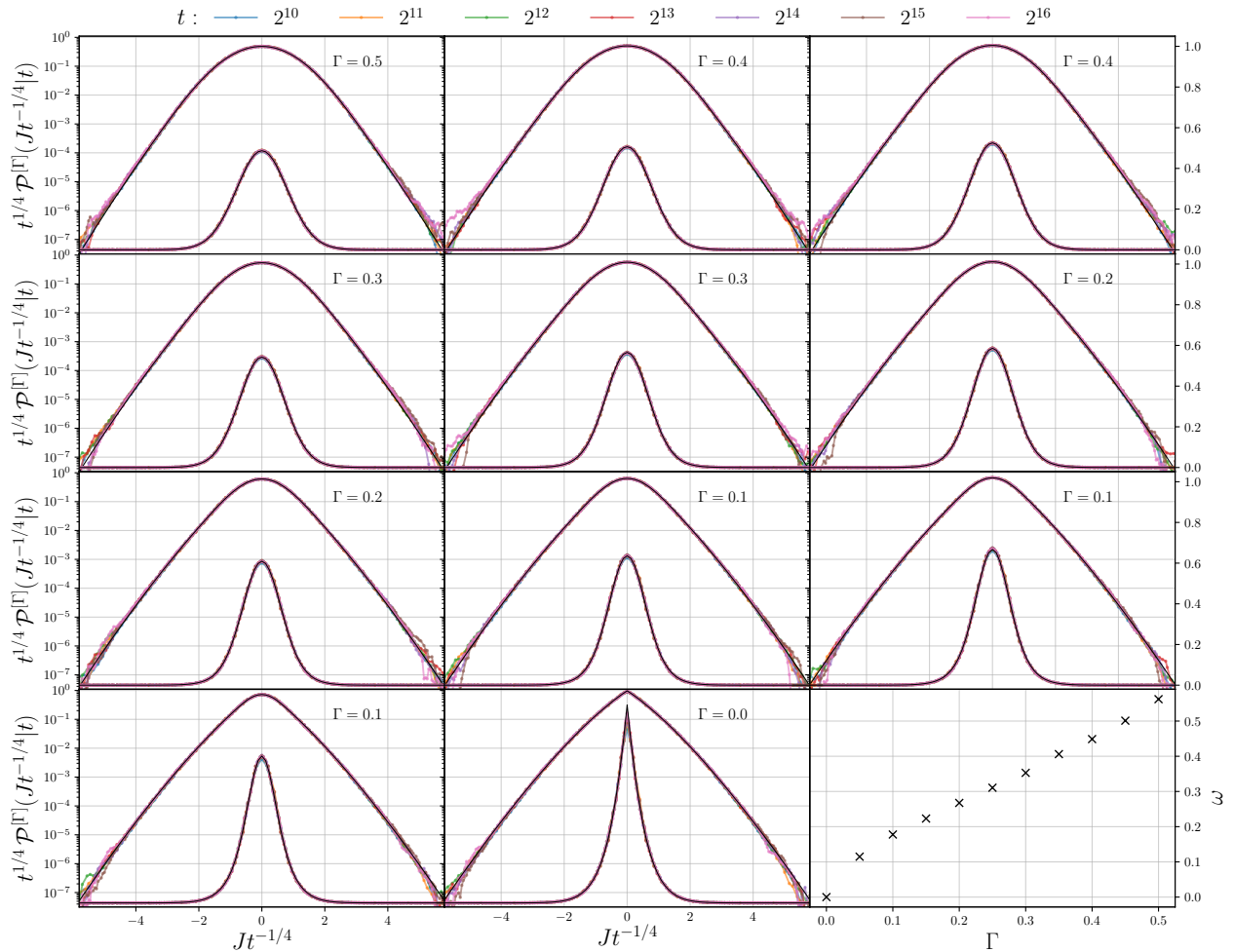


FIG. S2. Finite-type distributions of the charge integrated current $t^{1/4}\mathcal{P}^{[\Gamma]}(Jt^{-1/4}|t)$ (colored lines) on the typical scale in linear and logarithmic scales at additional values of the crossing parameter Γ compared to the main text. Black lines show best fits of asymptotic distributions of the form (S111) with ω and σ as fitting parameters, best-fit values reported in Table S1 (bottom right) Fitting parameter ω as a function of Γ . Simulation parameters: $\rho = 1/2$, $b = 0$, $L = 2^{20}$, $t_{\max} = 2^{16}$, 5×10^3 samples.

-
- [1] M. Medenjak, G. Policastro, and T. Yoshimura, $T\bar{T}$ -Deformed Conformal Field Theories out of Equilibrium, *Phys. Rev. Lett.* **126**, 121601 (2021).
- [2] Ž. Krajnik, J. Schmidt, V. Pasquier, E. Ilievski, and T. Prosen, Exact Anomalous Current Fluctuations in a Deterministic Interacting Model, *Phys. Rev. Lett.* **128**, 160601 (2022).
- [3] B. Doyon, G. Perfetto, T. Sasamoto, and T. Yoshimura, Ballistic macroscopic fluctuation theory, *SciPost Phys.* **15**, 136 (2023).
- [4] B. Doyon and J. Myers, Fluctuations in Ballistic Transport from Euler Hydrodynamics, *Annales Henri Poincaré* **21**, 255–302 (2019).

| Γ | 0.00 | 0.05 | 0.10 | 0.15 | 0.20 | 0.25 | 0.30 | 0.35 | 0.40 | 0.45 | 0.50 |
|----------------------|------|------|------|------|------|------|------|------|------|------|------|
| $\omega \times 10^1$ | 0.00 | 1.15 | 1.78 | 2.23 | 2.67 | 3.11 | 3.53 | 4.06 | 4.49 | 5.01 | 5.62 |
| $\sigma \times 10^1$ | 4.98 | 4.92 | 4.85 | 4.78 | 4.72 | 4.66 | 4.60 | 4.51 | 4.49 | 4.42 | 4.32 |

TABLE S1. Fitted values of ω and σ in the typical distribution (S111) as functions of the crossing parameter Γ . Simulation parameters as in Figure S2.

- [5] J. Myers, M. J. Bhaseen, R. J. Harris, and B. Doyon, Transport fluctuations in integrable models out of equilibrium, *SciPost Phys.* **8**, 007 (2020).
- [6] G. D. V. Del Vecchio, M. Kormos, B. Doyon, and A. Bastianello, Exact Large-Scale Fluctuations of the Phase Field in the Sine-Gordon Model, *Phys. Rev. Lett.* **131**, 263401 (2023).
- [7] K. Klobas, M. Medenjak, and T. Prosen, Exactly solvable deterministic lattice model of crossover between ballistic and diffusive transport, *Journal of Statistical Mechanics: Theory and Experiment* **2018**, 123202 (2018).
- [8] Private communication.
- [9] M. Medenjak, J. D. Nardis, and T. Yoshimura, Diffusion from convection, *SciPost Phys.* **9**, 075 (2020).